Volume 48
Number 27
21 July 2024
Pages 12067–12462

NJC

New Journal of Chemistry

A journal for new directions in chemistry

rsc.li/njc

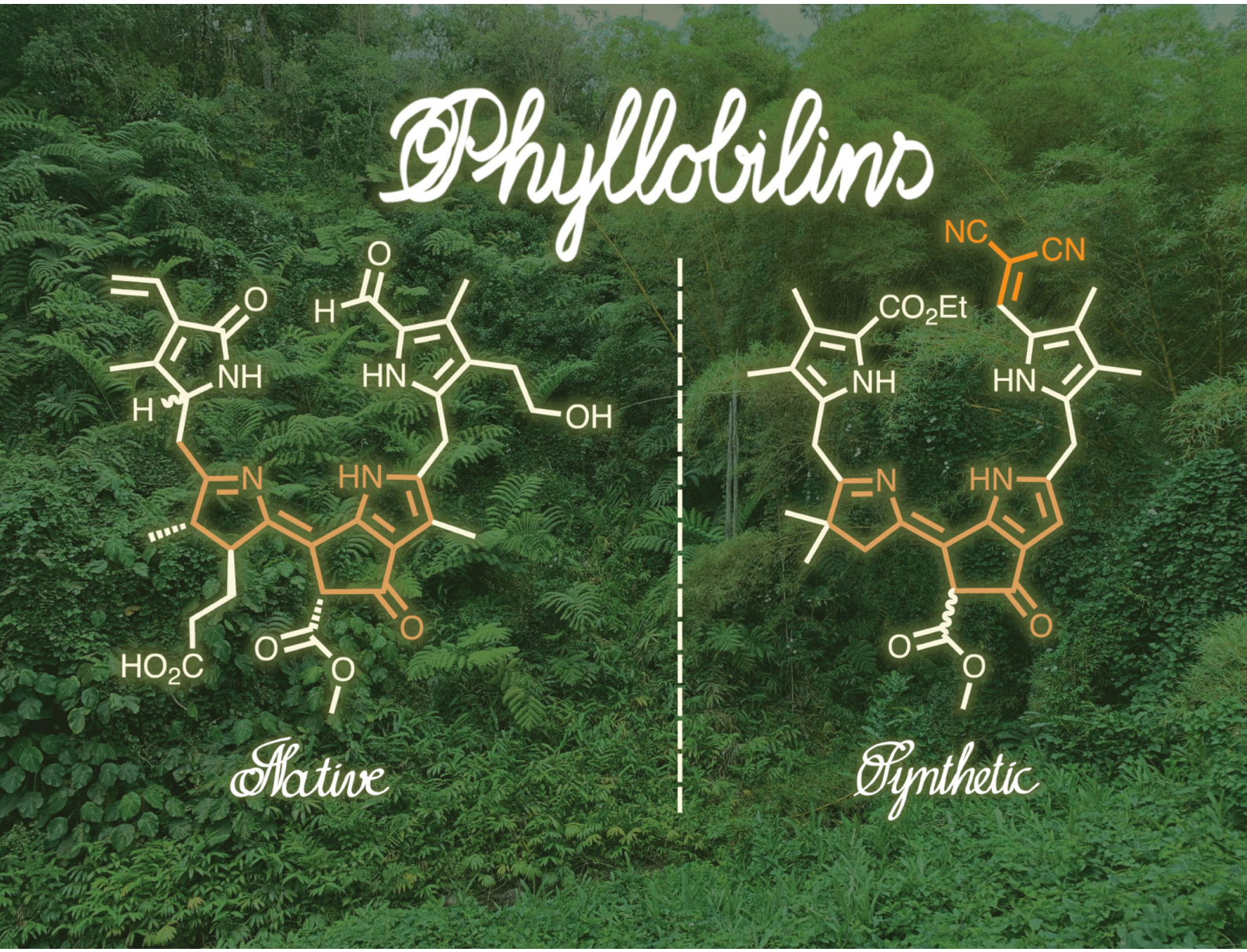

ISSN 1144-0546

ROYAL SOCIETY OF CHEMISTRY

PAPER
Anh Thu Nguyen Tran *et al.*
Synthesis of a model phyllobilin bearing an optical marker

cnrs

NJC

ROYAL SOCIETY OF CHEMISTRY

PAPER

View Article Online
View Journal | View Issue

Cite this: *New J. Chem.*, 2024, **48**, 12091

Synthesis of a model phyllobilin bearing an optical marker†

Anh Thu Nguyen Tran, [a] Pengzhi Wang, [a] Shaofei Zhang, [a] Milena Jovanovic, [a] Bianka Siewert, [b] Simone Moser [b] and Jonathan S. Lindsey *[a]

Received 2nd April 2024,
Accepted 29th May 2024

DOI: 10.1039/d4nj01533a

rsc.li/njc

Phyllobilins, derived from the breakdown of chlorophyll in plants, are acyclic tetrapyrroles that bear the signature ring E of the parent macrocycle. Few synthetic studies have concerned members of this emergent class of natural products, which now number >70. A prior synthesis of southern rim structures relied on Knoevenagel and Nazarov reactions to construct a dipyrromethane bearing the annulated ring E. Here, the synthesis has been extended to linear tetrapyrroles containing ring E as well as an appended dicyanovinyl unit. The latter serves as an optical marker with clearly observable absorption near 400 nm, rendering all compounds yellow, orange or red, thereby facilitating isolation and reaction monitoring. Knoevenagel condensation was carried out with a DC half (*gem*-dimethyl-substituted dihydrodipyrrin-1-carboxaldehyde bearing a 9-carboethoxy group) and an AB half (dipyrromethane equipped with a β-ketoester at the 8-position and the dicyanovinyl group at the 1-position). The resulting propenone is blocked by the ester and dicyanovinyl groups from reactions at the respective pyrrolic termini. Subsequent $Yb(OTf)_3$-catalyzed Nazarov reaction accompanied by unexpected prototropic rearrangement afforded the isolated phyllobilin (**8**) wherein conjugation shifted from the DC dihydrodipyrrin moiety to the CB southern rim, thereby resembling the conjugation of a native phyllolumibilin. The expected direct products of Nazarov cyclization, the *cis* and *trans* products (**pre-8-*cis***, **pre-8-*trans***) due to the configuration of substituents in ring E, were not observed. Calculations by density functional theory showed the stability order as **8** > **pre-8-*trans*** > **pre-8-*cis***. Access to phyllobilin analogues may open opportunities for fundamental studies pertaining to the native constituents, which are germane to plant sciences, nutrition, and ecology.

Introduction

Chlorophylls *a* and *b* are the chief light-harvesting pigments in plants. The annual production of such chlorophylls is estimated to be 10^{15} g.[1] The breakdown products of chlorophylls until recently were unknown – chlorophyll was regarded as simply vanishing in the global ecosphere. In the past 35 years, the chlorophyll breakdown process has begun to be characterized and found to entail oxidative scission of the macrocycle and companion transformations to yield a class of products known as phyllobilins. The companion reactions include oxidation and/or reduction of the π-system as well as modification of the peripheral substituents. More than 70 phyllobilins have been identified, which generally are acyclic tetrapyrroles that retain the telltale annulated ring of the parent chlorophyll *a* (Chart 1).[2–4] The phyllobilins have been grouped into categories on the basis of optical properties and corresponding molecular structures. Two general classifications originate on the basis of the structure of ring A: type I comprises an α-formylpyrrole unit whereas type II comprises an α-pyrrolinone unit (containing an α-oxo rather than α-formyl substituent). Within each type are subgroups of phyllolumibilins (and side-chain modified derivatives), phylloleucobilins, phylloxanthobilins, and phylloroseobilins. Examples of type I phyllobilins are shown in Chart 1. It warrants mention that the numbering system for phyllobilins is different from that of the parent chlorophylls.

For some time, phyllobilins were suspected to be mere catabolites of little interest. Recent studies, however, have revealed antioxidant,[5,6] anti-inflammatory,[7,8] and anti-proliferative[9] activities among the diverse phyllobilin family. Phenotypic

[a] *Department of Chemistry, North Carolina State University, Raleigh, NC 27695-8204, USA. E-mail: jlindsey@ncsu.edu; Tel: 919-515-6406*
[b] *Department of Pharmacognosy, Institute of Pharmacy, University of Innsbruck, Center for Chemistry and Biomedicine, Innsbruck 6020, Austria*

† Electronic supplementary information (ESI) available: Absorption spectra and determination of the molar absorption coefficients for **2** and **5–8**; ^{1}H NMR and $^{13}C\{^1H\}$ NMR data for all new compounds; single-crystal X-ray diffraction data. CCDC 2341280 (**2**). For ESI and crystallographic data in CIF or other electronic format see DOI: **https://doi.org/10.1039/d4nj01533a**

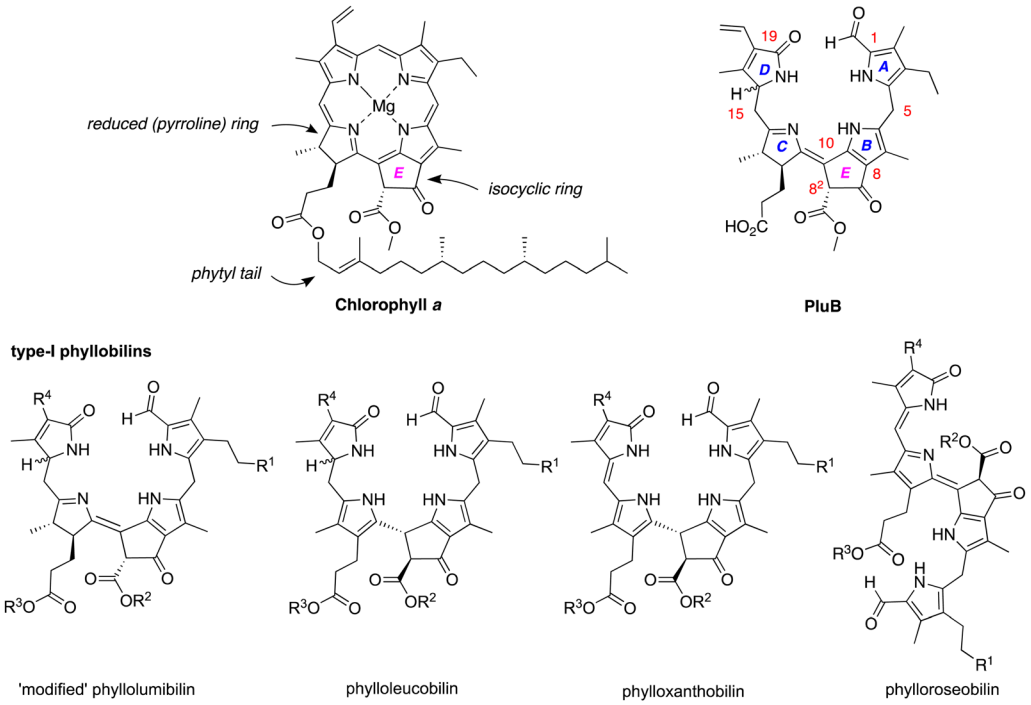

Chart 1 Structures of chlorophyll *a* and representative phyllobilins. The general nomenclature and numbering system for phyllobilins, illustrated for **PluB**, is shown at upper right.

screening for anti-migratory action in cancer cells has revealed actin as a protein target for phyllobilins.[10] Phyllobilins are thus an interesting class of natural products from phytochemical, biochemical, and photophysical viewpoints.[8,11] The evolutionary origin of the chlorophyll degradation pathway is proposed to have occurred commensurate with the emergence of land plants.[12] Despite their global abundance, ecological relevance, and potential human benefits in a plant-based diet, none of the known phyllobilins has yet been synthesized.

Both classes of natural products – chlorophylls and phyllobilins – have been relatively neglected as targets of chemical synthesis.[13] Studies of phyllobilins have remained dependent on isolation from natural sources, which typically has entailed laborious fractionation procedures. As part of a program to develop a total synthesis of native (bacterio)chlorophylls[14–19] and natural products derived therefrom such as phyllobilins, we have carried out a number of model studies to better understand the constraints associated with new synthetic routes. A model bacteriochlorophyll has been accessed *via* Knoevenagel condensation of two dihydrodipyrrins (**I**, **II-DHDP**) to form an enone (**III-BC**), which upon one-flask reaction undergoes Nazarov cyclization, electrophilic aromatic substitution, and elimination of methanol to yield the tetrapyrrole macrocycle bearing the annulated ring (isocyclic ring E) (Scheme 1, top panel).[14] Application of one dihydrodipyrrin (**I**) and one dipyrromethane (**II-DPM**) afforded enone **III-C** and the model chlorophyll (Scheme 1, middle panel).[15] A more recent study employed a pyrrole-carboxaldehyde (**IV**) and pyrrole-β-ketoester (**V**) to form the enone (**VI**), which upon Nazarov cyclization afforded the annulated dipyrromethane (**VII**) (Scheme 1, bottom panel).[20] The products resemble the southern rim of phylloleucobilins and phylloxanthobilins (Chart 1). The Knoevenagel condensation of **IV** and **V** gave reasonable yields (43–92%). The Nazarov cyclization of compound **VI** in the presence of 2,6-di-*tert*-butylpyridine (2,6-DTBP), $In(OTf)_3$, and $LiClO_4$ at 40–50 °C afforded the southern rim structure **VII** in 51–80% yield.

This paper reports an extension of the strategies shown in Scheme 1 to prepare a model phyllobilin. The model phyllobilin contains a *gem*-dimethyl group, rather than a *trans*-dialkyl group, in the pyrroline ring. The tetrapyrrolic intermediate formed upon Nazarov cyclization underwent unexpected *in situ* prototropic rearrangement to obtain a southern rim architecture similar to that of native type-I phyllolumibilins. The long-term objective of the work described herein is to gain access to diverse phyllobilins for fundamental chemical, ecological, and nutritional studies.

Results and discussion

Synthesis of a dipyrromethane bearing a 2,2-dicyanovinyl group

To study the formation of phyllobilin-like compounds, targets were sought that contain four pyrrolic rings yet also are equipped with a marker for visible absorption spectroscopic monitoring. For the latter objective, the 2,2-dicyanovinyl moiety attached to a pyrrole was attractive. The 2,2-dicyanovinyl unit was first employed nearly a century ago in the chemistry of pyrroles,[21] and was later used by Rapoport in the synthesis of deoxophylloerythroetioporphyrin.[22] Woodward also reported the use of the 2,2-dicyanovinyl unit in the synthesis toward

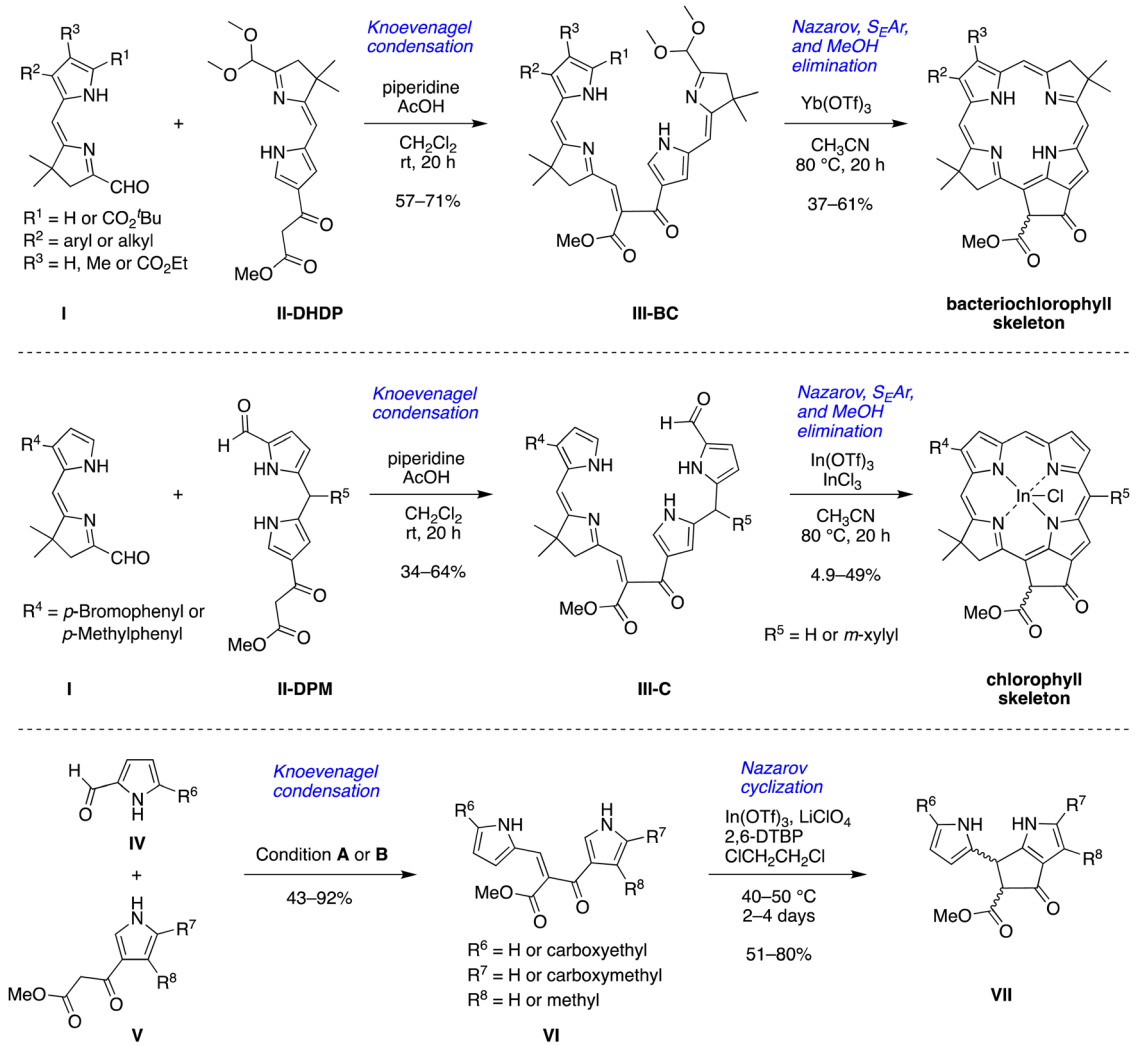

Scheme 1 Routes to the skeleton of bacteriochlorophylls, chlorophylls and southern rim structures. Condition **A**: piperidine, AcOH, MS 4 Å, CH_2Cl_2, 40 °C, 20 h; condition **B**: piperidine, MeOH, 50 °C, 24 or 48 h.

chlorophyll as a masked formyl group of the ring B pyrrole.[23] Subsequent use has been sparing,[24–30] with applications in the synthesis of porphocyanines[31] and dipyrromethanes.[32–37] The sparing use may stem from the emergence of diverse protecting groups for pyrroles[38] and the challenges of deprotection of the dicyanovinyl group. Previous reports relied solely on absorption spectroscopy for characterization of pyrroles bearing a 2-(2,2-dicyanovinyl) substituent.[22,23] The 2,2-dicyanovinyl moiety is inert under acidic and other conditions,[38] which is attractive for use in synthesis as described in the following.

Pyrroles **1**,[39,40] **2**,[25] and **3**[25] are known compounds. Pyrrole **3** was previously prepared from 2-ethoxycarbonyl-3,4,5-trimethylpyrrole.[25] Here, a new route to pyrrole **3** was developed from inexpensive *tert*-butyl acetoacetate (Scheme 2). Treatment of *tert*-butyl acetoacetate with sodium nitrite solution in acetic acid followed by addition of 3-methyl-2,4-pentanedione and zinc dust[39] gave pyrrole **1** in 50% yield. Treatment of **1** with benzoyl chloride in DMF at reflux gave 2-formyl-3,4,5-trimethylpyrrole, which upon reaction with malononitrile in ethanol at 70 °C afforded 2-(2,2-dicyanovinyl)pyrrole **2** in 43% yield over the two steps.[25] Pyrrole **2** was charactered by single-crystal X-ray diffraction (see the ESI†). Chlorination of **2** with sulfuryl chloride in acetic acid at 55 °C[25] yielded pyrrole **3** in 73% yield upon simple filtration.

The condensation[41] of 5-chloromethyl-2-(2,2-dicyanovinyl)-pyrrole **3** and known β-ketoester-substituted pyrrole **4**[17] in CH_2Cl_2 containing $SnCl_4$ afforded dipyrromethane **5** in 35% yield. Other reported acidic conditions, such as refluxing HCl/ethanol,[23] led to hydrolysis of the ester and cleavage of the carboxylic acid, thereby converting the β-ketoester to an acetyl group (not shown). The absorption spectra of the 2,2-dicyanovinyl-substituted compounds **2**, **3**, and **5** are shown in Fig. 1. The 2,2-dicyanovinyl chromophore is responsible for the strong absorption peak at 403 nm, 389 nm and 402 nm of **2**, **3**, and **5**, respectively.

Formation of a model phyllobilin

Knoevenagel condensation[42,43] of dipyrromethane **5** and known dihydrodipyrrin–carboxaldehyde **6**[44] in the presence of

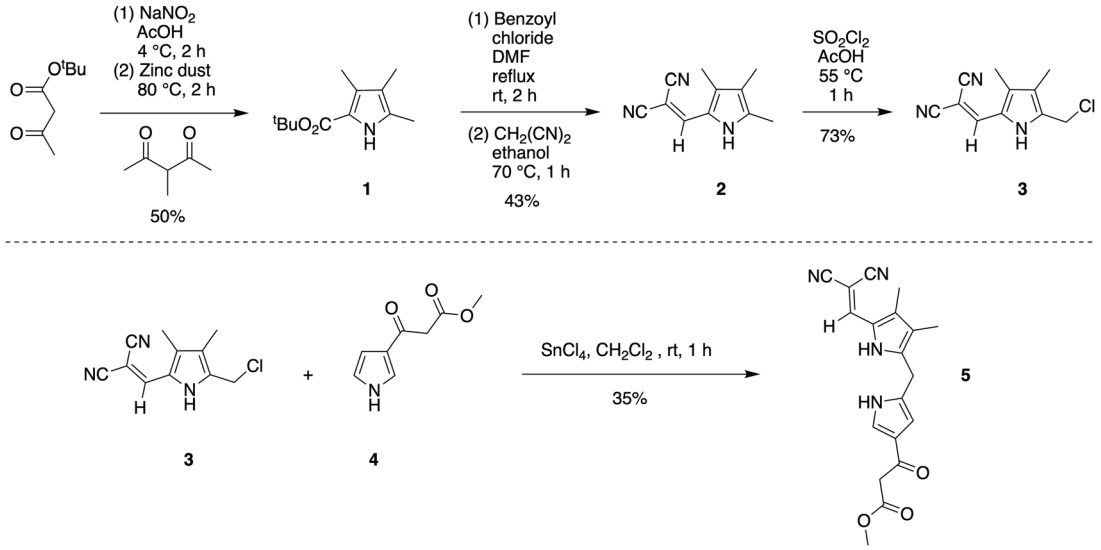

Scheme 2 Synthesis of 2,2-dicyanovinyldipyrromethane **5**.

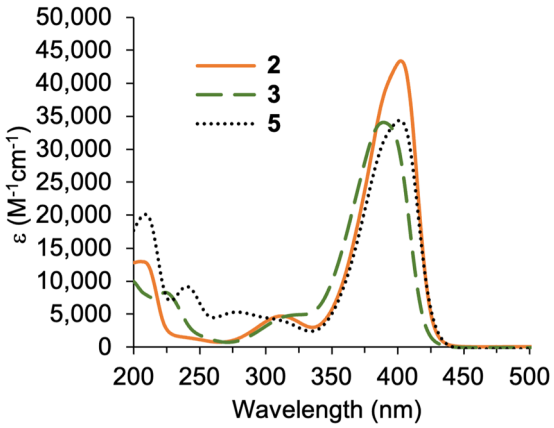

Fig. 1 Absorption spectra in acetonitrile at room temperature of **2**, **3**, and **5**.

AcOH/piperidine gave the desired α,β-unsaturated ketone **7** in 31% yield (Scheme 3). The stereochemical configuration of the alkene in **7** could not be determined unambiguously. The *E* isomer is often formed preferentially in Knoevenagel reactions of heteroaromatic β-keto esters; regardless, interconversion of the *E* and *Z* isomers occurs during the course of the Nazarov cyclization.[16,17,45] Subsequent Nazarov cyclization[45–47] catalyzed by $Yb(OTf)_3$ afforded phyllobilin **8** in 46% yield. The yield was consistent with the tetrapyrrole intermediates that typically gave bacteriochlorins (*via* Nazarov, S_EAr, and methanol elimination) in ~50% yield.[14–16] However, the previous conditions for the double-ring closure employed ten equivalents of the Lewis acid ($Yb(OTf)_3$),[14] whereas here the cyclization of enone **7** only required one equivalent of $Yb(OTf)_3$. The Nazarov reaction of enone **7** with ten equivalents of $Yb(OTf)_3$ afforded phyllobilin **8** in only 11% yield (not shown). The model phyllobilin **8** was characterized by NMR spectroscopy, ESI-MS, and absorption spectroscopy.

The absorption spectra of enone **7** and model phyllobilin **8** are shown in Fig. 2. The distinct peaks allowed the reaction to be monitored by absorption spectroscopy. Thus, the time course of the transformation of **7** to **8** (one equivalent of $Yb(OTf)_3$) was monitored by removal of 50 μL samples from the reaction mixture ([**7**] = 0.2 mM initially), dilution to 1 mL, and analysis by absorption spectroscopy. The spectral evolution is shown in Fig. 2. The key features are as follows: (1) within 5 min upon treatment with $Yb(OTf)_3$, the peak at 468 nm declined along with those at ~403 and 279 nm. The disappearance of the peak at 468 nm, which is characteristic of the

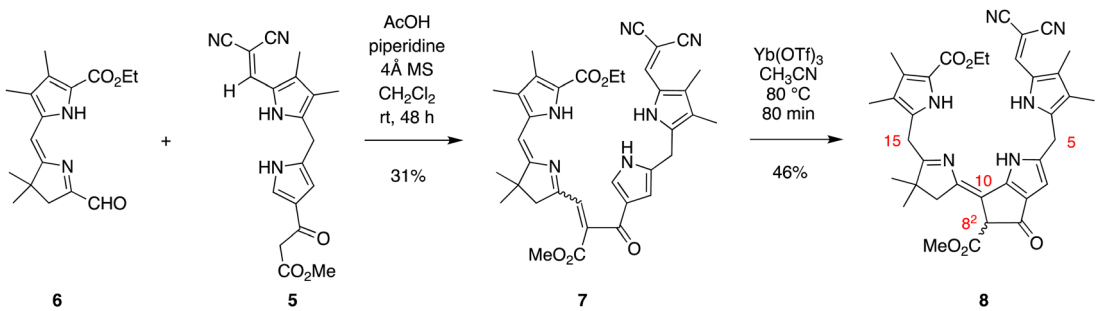

Scheme 3 Synthetic route to a model phyllobilin.

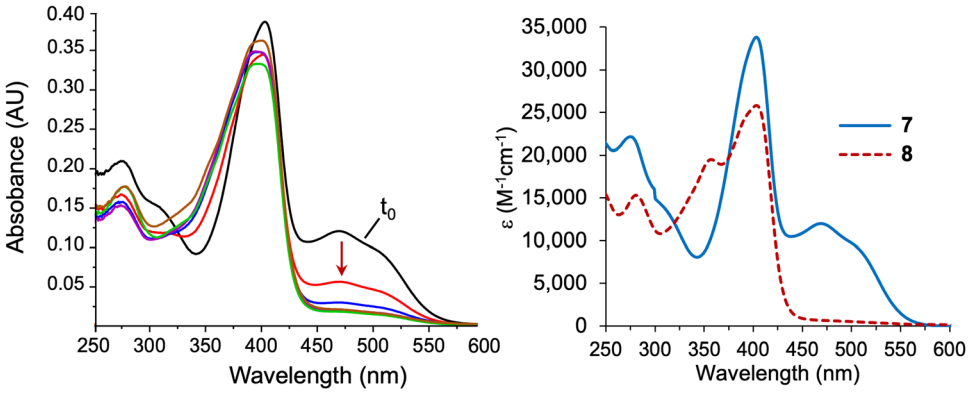

Fig. 2 Absorption spectra in acetonitrile at room temperature. Left: Time-course spectral evolution of the conversion of **7** to **8** upon treatment under the Nazarov cyclization (0 min, black; 5 min, red; 10 min, blue; 20 min, magenta; 40 min, green; 80 min, brown). Right: Purified **7** and **8**.

enone π-system, reflects the ring closure of the Nazarov reaction, which affords a saturated center at position 8^2. (2) A broad peak at ~350 nm gradually arose after 5 min and also reached a maximum after 80 min. (3) The absorption spectrum observed at 80 min remained constant for a subsequent hour (not shown). All of the time-evolution traces are provided in the ESI.†

Characterization

Enone **7** and model phyllobilin **8** were examined by ^{1}H NMR spectroscopy including COSY and NOESY analysis. Expected features in the ^{1}H NMR spectra of **7** and **8** are as follows (Fig. 3): (i) Each spectrum revealed signals corresponding to 38 protons. Among the signals are seven singlets due to the seven methyl groups. The four methyl groups on the two Northern pyrroles of both appear as four singlets in the region δ = 2.0–2.3 ppm. The two methyl groups of the *gem*-dimethyl moiety in phyllobilin **8** (δ = 1.25 and 1.27 ppm) are diastereotopic owing to the stereocenter in the isocyclic ring (position 8^2) while the two methyl groups are equivalent in enone **7** (δ = 1.08 ppm). (ii) The methylene unit at position 12 in model phyllobilin **8** resonates as AB peaks (δ = 2.42–2.44 and 2.53–2.55 ppm) due to the stereocenter at position 8^2, while that of enone **7** appears as a singlet (δ = 2.48 ppm). (iii) The *meso* methylene unit at position 5′ in enone **7** appears as a singlet at δ = 3.99 ppm, whereas that

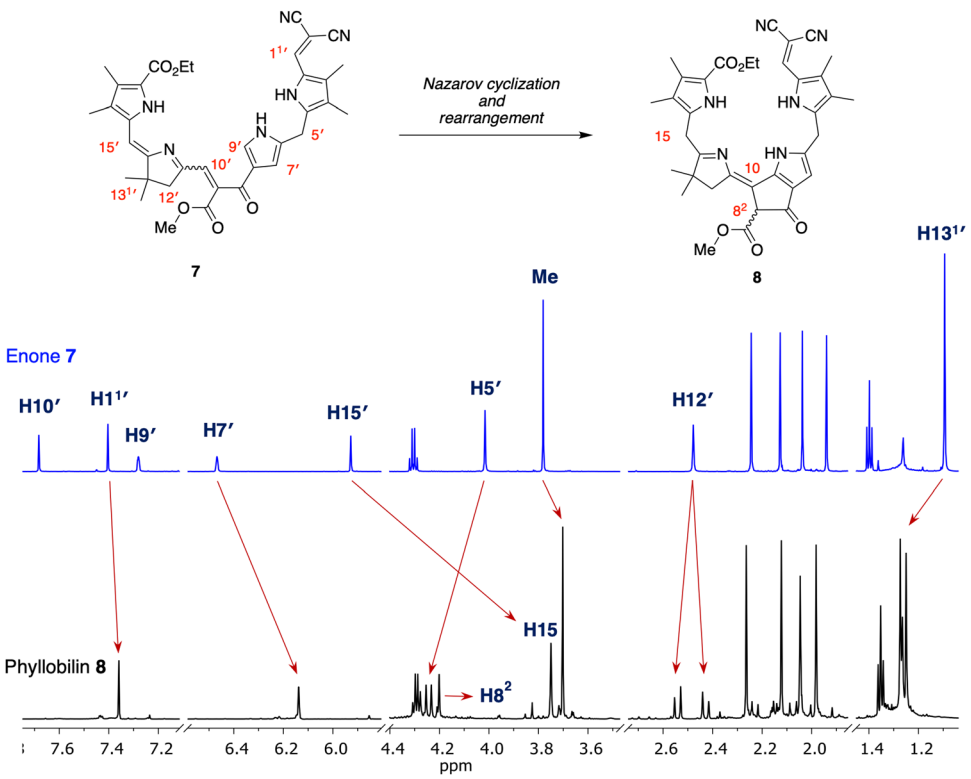

Fig. 3 Correspondence of ^{1}H NMR spectra (in CD_2Cl_2 at room temperature, 700 MHz) of reactant **7** (top) and isolated product **8** (bottom).

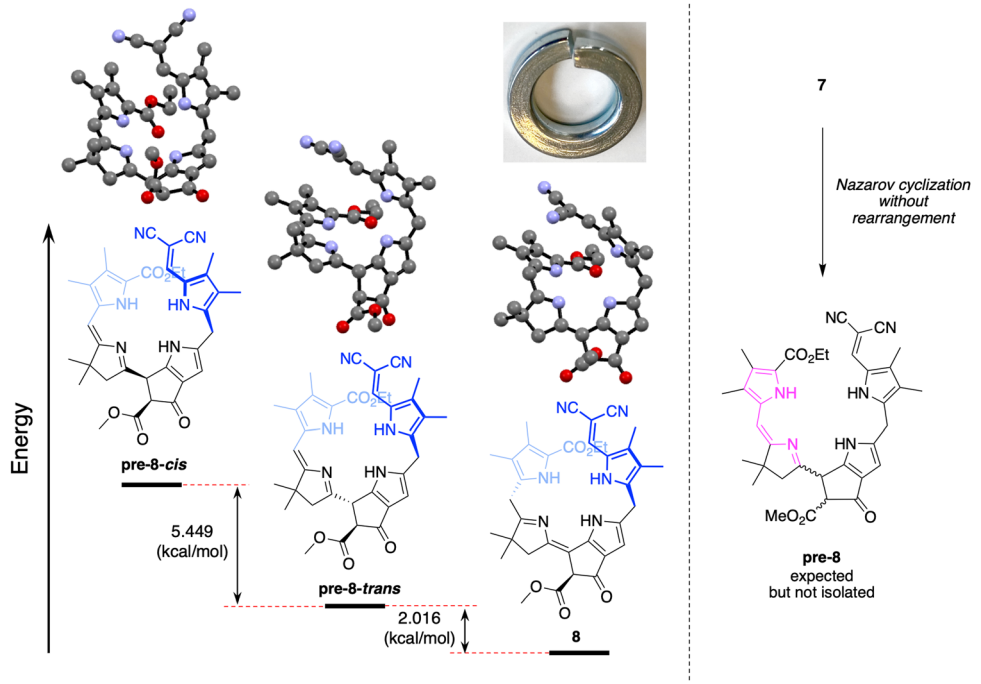

Fig. 4 Optimized structures of compound **pre-8-*cis***, **pre-8-*trans*** and **8** (hydrogen atoms omitted for clarity); a picture of a lock washer; and scheme showing expected formation of **pre-8** upon Nazarov cyclization of **7**.

at position 5 of model phyllobilin **8** appears as a doublet at δ = 4.25 ppm (with a nOe observed with the proton at position 7).

On the other hand, key unexpected features are as follows: (i) The resonance due to the *meso* proton at position 15′ in enone **7** (δ = 5.89 ppm) is not seen in model phyllobilin **8**, which instead shows an upfield resonance (δ = 3.70 ppm) due to two protons. (ii) The resonance due to the methine at position 9′ in enone **7** disappears as expected in model phyllobilin **8**. On the other hand, the signal due to the proton at position 10′ in enone **7** is unexpectedly missing in model phyllobilin **8**. (iii) The proton at position 8^2 of **8** is observed at δ = 4.20 ppm, consistent with the β-ketoester motif of the phyllobilin, but resonates as a singlet. (iv) A COSY spectrum of **8** shows no interaction between other protons and the proton at position 8^2, indicating the absence of a proton at the adjacent *meso*-carbon (position 10). (v) A NOESY spectrum of **8** shows interaction between the *gem*-dimethyl protons and the two protons at position 15. The spectral data are consistent with saturation at position 15 and unsaturation at position 10, which can only occur upon prototropic rearrangement (*i.e.*, double-bond migration) following Nazarov cyclization.

Density functional theoretical (DFT) calculations[48] were carried out to gain insight concerning the driving force for the prototropic rearrangement. Three compounds were considered: the isolated product **8** and the two expected products upon Nazarov cyclization without rearrangement, **pre-8-*trans***, and **pre-8-*cis***. The geometry optimization was performed at the PBE0/def2-TZVP level of theory[49–51] using Orca 5.0.4[52] in vacuum at 0 K. Note that each compound **8**, **pre-8-*trans***, and **pre-8-*cis*** has an enantiomer (not shown), which were not the subject of calculation. The optimized structures of **pre-8-*cis***, **pre-8-*trans*** and **8** are shown in Fig. 4. Each compound exhibited a somewhat helical architecture, like that of a lock washer, which is not unexpected given the constrained geometry of the southern rim and the presence of two appended pyrrole units

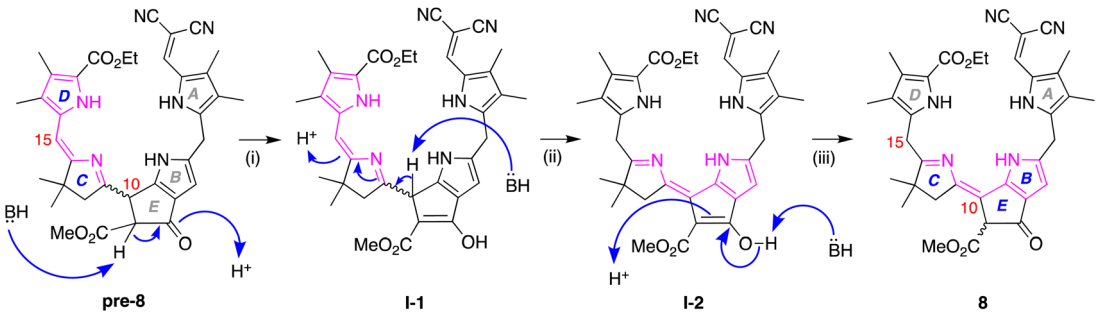

Scheme 4 Proposed rearrangement pathway leading to model phyllobilin **8**.

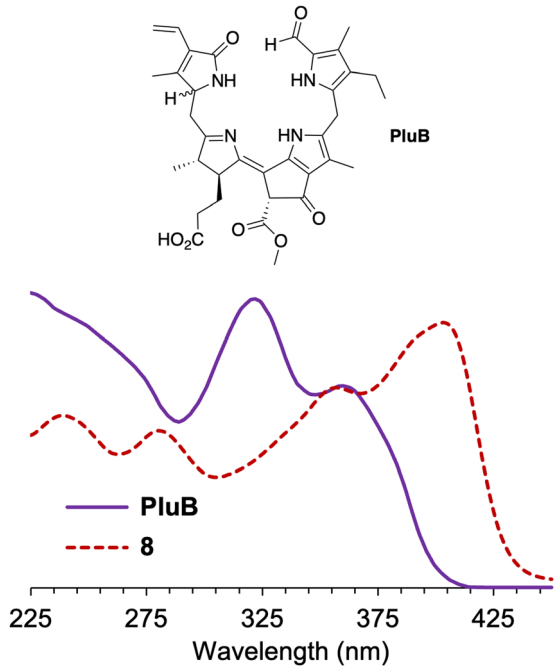

Fig. 5 Absorption spectra at room temperature of phyllolumibilin **PluB**[4] in aqueous MeOH (potassium phosphate buffer, 20 mM, pH 7) and **8** in acetonitrile (normalized at 355 nm).

(indeed, helical chirality is known for bilins.[53]). The results showed the order of stability to be **8** > **pre-8-*trans*** > **pre-8-*cis***. The difference in energy between **8** and **pre-8-*trans*** is 2.016 kcal mol^{-1}, while that of **pre-8-*trans*** and **pre-8-*cis*** is 5.449 kcal mol^{-1}. Hence, the final product **8** is predicted to be energetically favored, which is consistent with experimental observation.

The prototropic rearrangement in model phyllobilin **8** in effect shifts the double bond from the dihydrodipyrrin constituent (originating in **6**) to the lower rim. In other words, the dihydrodipyrrin unit has shifted from encompassing rings DC to rings CB. The mechanism is not known. While a simple mechanism would entail abstraction of the proton at position 10 (H^{10}), forming an enamino structure, a more interesting mechanism may involve the more acidic proton of the β-ketoester. A corresponding formal mechanism is outlined in Scheme 4 as one proposal. In step (i), keto–enol tautomerism of the β-ketoester of **pre-8** affords **I-1**. In step (ii), abstraction of H^{10}, which is allylic, benzylic, and located at the imine α-position, may trigger the prototropic rearrangement to give **I-2**. In step (iii), the enol reverts to the β-ketoester. The two keto–enol tautomeric processes (steps (i) and (iii)) are expected to be reversible, whereas the conversion of **I-1** to **I-2** in step (ii) is likely to be the source of exergonicity. While the keto–enol tautomerism of the β-ketoester of chlorophylls and related macrocycles has been examined over several decades,[54–58] more in-depth calculations would be required to provide insight concerning possible mechanisms.

The normalized absorption spectrum of a native phyllolumibilin (**PluB**)[4] and model phyllobilin **8** are shown in Fig. 5. The native and synthetic compounds share a similar absorption peak at ~355 nm. The absorption band near 355 nm is a feature in common with the B/C chromophore of fluorescent chlorophyll catabolites, such as **PluB**[4]. The typical absorption

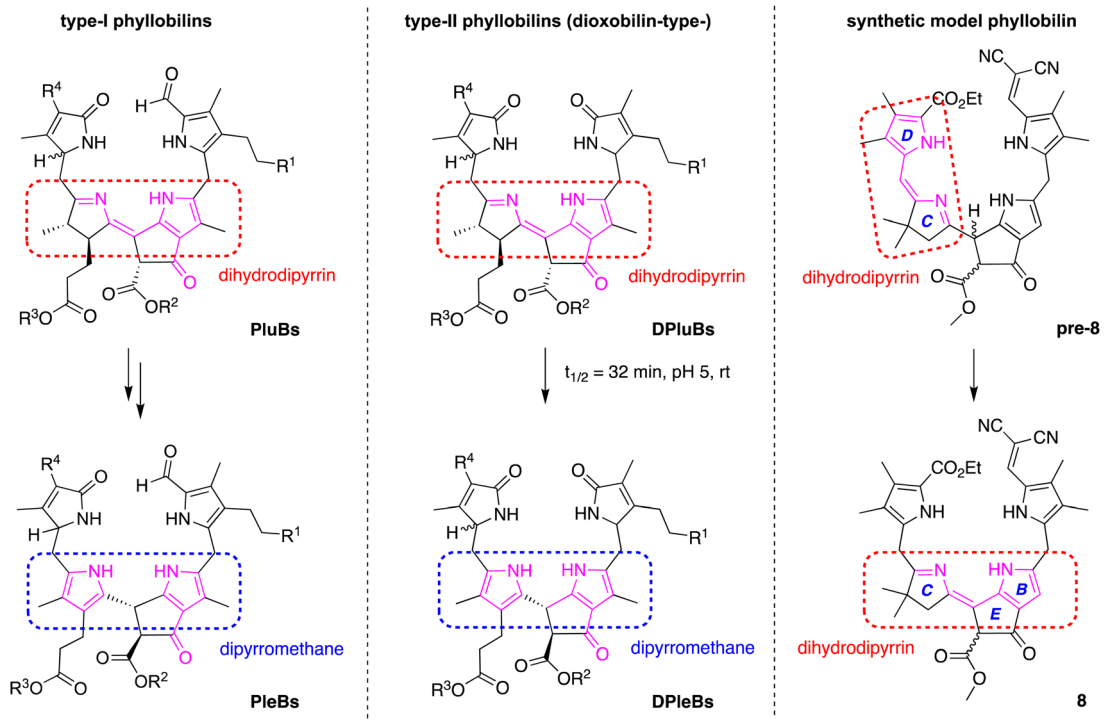

Scheme 5 Natural phyllobilins and a synthetic phyllobilin.

(312 nm) for the α-formylpyrrole unit (ring A) in phyllolumibilins is absent in **8**, replaced instead by the absorption at 403 nm corresponding to the α-(2,2-dicyanovinyl)pyrrole unit.

The structures of typical native phyllobilins[59–62] are shown in Scheme 5. The formation of the native phyllobilins begins with chlorophyll *a* and proceeds *via* oxidation and reduction to give the observed products. For example, phyllolumibilins (**PluBs**), which contain a dihydrodipyrrin chromophore encompassing rings B and C, undergo double prototropic rearrangement upon treatment with acid to give the dipyrromethane wherein the pyrroline ring has become unsaturated (Scheme 5, left panel). In so doing, the *trans*-dialkyl stereochemistry of ring C is lost. Similarly, spontaneous rearrangement of dioxophyllolumibilins (**DPluBs**) converts the pyrroline to a pyrrole and saturates position 10 to give the dioxophylloleucobilins (**DPleBs**, Scheme 5, middle panel).[62] For conversion of expected product **pre-8** to the isolated model phyllobilin **8**, the *gem*-dimethyl group at position 13 precludes the tautomerization involving the β-position of the pyrroline motif; instead, the tautomerization engages with the flanking *meso* site (position 15) (Scheme 4). Thus, due to the *gem*-dimethyl group at the 13-position in **8**, isomerization typical in the natural system that converts a phyllolumibilin to a phylloleucobilin, or a dioxophyllolumibilin to a dioxophylloleucobilin, is not possible.

Conclusions

A route toward a synthetic phyllobilin has been developed *via* Knoevenagel condensation of a dihydrodipyrrin-carboxaldehyde (DC half) and a dipyrromethane-β-ketoester (AB half) followed by Nazarov cyclization. The route has been extended from that under investigation for the total synthesis of native (bacterio)chlorophylls. The A and D pyrroles (of the respective AB and DC halves) bear substituents at the α-positions to block reactions. The dicyanovinyl group blocks macrocyclization and provides a convenient chromophore (~400 nm) that facilitates compound isolation and reaction monitoring. The synthetic phyllobilin contains the characteristic BCE ring architecture of native phyllobilins. The π-conjugation resembles a phyllolumibilin and forms by prototropic rearrangement following Nazarov cyclization. Further studies will be required to gauge the general occurrence of such rearrangements, which heretofore seem to have not been described. On the other hand, several distinctions from the native structures include (1) the presence of a *gem*-dimethyl group in pyrroline ring C, (2) a tetrahydrodipyrrin π-system encompassing rings C and D, and (3) methyl groups at four β-positions of the pyrroles. A present limitation is the low yield of the Nazarov cyclization. The synthetic work provides an entrée for further studies related to the chemistry of phyllobilins, which ultimately impinges on the fields of plant biology, nutrition, ecology, and agricultural sciences.

Experimental section

General methods

^{1}H NMR and ^{13}C NMR spectra were collected at room temperature in $CDCl_3$ unless noted otherwise. Absorption spectra were collected in 1-cm pathlength quartz cuvettes at room temperature. Electrospray ionization mass spectrometry (ESI-MS) data are reported for the molecular ion or protonated molecular ion. Molecular sieves (4 Å, powder) were heated (120 °C) overnight prior to use. Silica (40 μm average particle size) was used for column chromatography. THF used in all reactions was freshly distilled from Na/benzophenone ketyl unless noted otherwise. THF (ACS-grade) was used as received. Solutions that were concentrated were done so under reduced pressure using a rotary evaporator. All commercially available compounds were used as received. Non-commercial and known compounds **1**,[39] **2**,[25] and **4**[18] were prepared as described in the literature. Known compound **3**[25] was prepared by a new route described herein.

Computational methods

Density function calculations were performed using Orca 5.0.4.[48] The geometry optimization calculations were done at the PBE0/def2-TZVP level of theory,[49–51] followed by frequency calculations at the same level of theory to confirm that all structures are true minima. The energies of **8**, **pre-8-*trans***, and **pre-8-*cis*** were −2097.720, −2097.717, and −2097.708 Hartree.

Synthesis

2-*tert*-Butyl-carboxylate-3,4,5-trimethylpyrrole (1). Following a reported procedure[39] at 2-fold larger scale, a solution of *tert*-butyl acetoacetate (63.2 g, 0.400 mol) in glacial acetic acid (160 mL) was treated with aqueous sodium nitrite solution (29.6 g, in 100 mL of deionized water). The resulting reaction mixture was stirred for 20 min at ~10 °C (ice bath), for 2 h at 4 °C, and overnight at room temperature. Then, 2-methyl-2,4-pentanedione (53.6 g, 0.400 mol) was added followed by zinc dust (56.0 g, 0.860 mol), with the temperature kept at ~80 °C (oil bath) during the addition. The reaction mixture was stirred for 30 min and then heated and stirred at 100 °C for 2 h. The hot mixture was poured into a 1 L beaker containing cold water, and the crude precipitate was separated. The precipitated solid was crystallized in hot ethanol to give a yellow solid (42 g, 50%): mp: 135–137 °C; ^{1}H NMR (500 MHz, $CDCl_3$) δ 1.56 (s, 9H), 1.91 (s, 3H), 2.18 (s, 3H), 2.23 (s, 3H), 8.61 (br s, 1H); ^{13}C{^{1}H} NMR (125 MHz, $CDCl_3$) δ 8.8, 10.7, 11.4, 28.6, 80.0, 116.9, 117.9, 126.6, 128.7, 161.4; HRMS (ESI-TOF) *m/z*: $[M + H]^+$ calcd for $C_{12}H_{20}NO_2$ 210.1489; found 210.1485.

2-(2,2-Dicyanovinyl)-3,4,5-trimethylpyrrole (2). Following a reported procedure,[25] a solution of **1** (22.3 g, 0.110 mol) in DMF (60 mL) at reflux (oil bath) was treated with a solution of benzoyl chloride (23 mL, 0.200 mol) in DMF (60 mL) over 2 min. The mixture was stirred for 10 min, and the imine salt crystallized when the reaction mixture was allowed to cool to room temperature for 2 h. The filtered solid was rinsed with DMF and then diethyl ether. The crude product was dissolved in water (30 mL) and filtered through a Celite pad. The dark-orange

filtrate was treated with aqueous ammonia (30%, 30 mL) and then heated to achieve recrystallization. The corresponding product was dissolved in CH_2Cl_2, washed with water, dried (Na_2SO_4) and concentrated to give 2-formyl-3,4,5-trimethylpyrrole (~7.5 g) as an orange–brown solid. A sample of the crude pyrrole (~6.8 g, 50 mmol) was directly dissolved in ethanol (150 mL) and then treated with malononitrile (3.6 g, 55 mmol) and diethylamine (50 mL). The reaction mixture was stirred overnight at 70 °C (oil bath). The reaction mixture was filtered to obtain the crude solid precipitate, which then was washed with ethanol to give a yellow solid (7.95 g, 43% over two steps): mp 176–178 °C; ^{1}H NMR (500 MHz, $CDCl_3$) δ 1.91 (s, 3H), 2.08 (s, 3H), 2.18 (d, J = 8.3 Hz, 1H), 2.27 (s, 3H), 9.28 (s, 1H); $^{13}C\{^1H\}$ NMR (125 MHz, $CDCl_3$) δ 8.7, 9.8, 12.5, 62.4, 116.2, 117.7, 120.7, 124.0, 136.8, 140.5, 141.3; HRMS (ESI-TOF) m/z: $[M + H]^+$ calcd for $C_{11}H_{12}N_3$ 186.1026; found 186.1024. UV-Vis λ_{max} (MeCN) (ε) 403 (nm) (43 000 M^{-1} cm^{-1}).

2-Chloromethyl-5-(2,2-dicyanovinyl)-3,4-dimethylpyrrole (3). Following a reported procedure[25] with modification, a solution of **2** (1.25 g, 6.75 mmol) in glacial acetic acid (40 mL) was treated dropwise with sulfuryl chloride (600 μL, 7.42 mmol) at 55 °C (oil bath). The resulting reaction mixture was stirred at 55 °C (oil bath) for 1 h and then allowed to cool to room temperature. The reaction mixture was filtered, and the filter cake was washed with glacial acetic acid and hexanes. The resulting solid was collected and dried under high vacuum to obtain a light-yellow solid (1.09 g, 73%): mp 172–175 °C dec.; ^{1}H NMR (600 MHz, $CDCl_3$) δ 2.03 (s, 3H), 2.15 (s, 3H), 4.60 (s, 2H), 7.44 (s, 1H), 9.53 (s, 1H); $^{13}C\{^1H\}$ NMR (150 MHz, $CDCl_3$) δ 8.7, 9.8, 36.0, 67.6, 115.2, 116.6, 121.4, 124.9, 136.0, 136.8, 142.2; HRMS (ESI-TOF) m/z: $[M + H]^+$ calcd for $C_{11}H_{11}ClN_3$ 220.0636; found 220.0633. UV-Vis λ_{max} (MeCN) (ε) 388 (nm) (34 000 M^{-1} cm^{-1}).

1-(2,2-Dicyanoethenyl)-8-(3-methoxy-1,3-dioxopropyl)-2,3-dimethyldipyrromethane (5). Following a reported procedure[41] with modification, a solution of pyrrole **3** (1.51 g, 6.88 mmol) and pyrrole **4** (1.04 g, 6.25 mmol) in anhydrous CH_2Cl_2 (60 mL) was cooled to 0 °C (ice bath) under argon. The reaction mixture was treated dropwise with $SnCl_4$ (850 μL, 7.3 mmol) at 0 °C. After stirring at room temperature for 1 h, the reaction mixture was poured into a beaker containing ice-water. The resulting mixture was extracted with ethyl acetate (3 × 100 mL). The organic extract was dried (Na_2SO_4) and concentrated to afford a brown paste. The paste was then washed with CH_2Cl_2 to obtain a yellow solid (843.5 mg, 35%): ^{1}H NMR (600 MHz, acetone-d_6) δ 1.98 (s, 3H), 2.21 (s, 3H), 3.63 (s, 3H), 3.76 (s, 2H), 4.17 (s, 2H), 6.38–6.39 (m, 1H), 7.54–7.55 (m, 1H), 7.73 (s, 1H), 9.95 (s, 1H), 10.69 (s, 1H); $^{13}C\{^1H\}$ NMR (150 MHz, acetone-d_6) δ 8.7, 9.7, 25.4, 46.8, 52.1, 64.1, 107.6, 116.8, 117.3, 121.2, 124.9, 125.7, 126.4, 130.1, 137.8, 142.5, 142.7, 169.1, 187.2; ESI-MS m/z: $[M + H]^+$ calcd for $C_{19}H_{19}N_4O_3$ 351.1452; found 351.1442. UV-Vis λ_{max} (MeCN) (ε) 400 (nm) (34 000 M^{-1} cm^{-1}).

3-[9-Carbethoxy-2,3-dihydro-3,3,7,8-tetramethylpyrrin-1-yl]-2-carbomethoxy-1-[9-(2,2-dicyanoethenyl)-7,8-dimethyldipyrromethan-2-yl]prop-2-ene-1-one (7). Following a reported procedure,[14] a mixture of dipyrromethane **5** (56.2 mg, 0.160 mmol), dihydrodipyrrin **6** (48.0 mg, 0.159 mmol), and dried molecular sieves 4 Å powder (129 mg) under argon was treated with a solution of piperidine/acetic acid in anhydrous CH_2Cl_2 (15 mM/15 mM, 3.2 mL). The reaction mixture was stirred at room temperature for 48 h. The reaction mixture was filtered through a Celite pad. The filtrate was concentrated and chromatographed [silica, hexanes/ethyl acetate (1 : 1)] to afford a red solid (29.9 mg, 31%): mp 160–165 °C; ^{1}H NMR (600 MHz, $CDCl_3$) δ 1.08 (s, 6H), 1.40–1.42 (t, J = Hz, 3H), 1.93 (s, 3H), 2.04 (s, 3H), 2.11 (s, 3H), 2.25 (s, 3H), 2.25 (s, 3H), 2.48 (s, 2H), 3.79 (s, 3H), 3.99 (s, 2H), 4.31–4.35 (q, J = Hz, 2H), 5.89 (s, 1H), 6.46 (s, 1H), 7.25 (s, 1H), 7.32 (s, 1H), 7.72 (s, 1H), 9.16 (s, 1H), 9.36 (s, 1H), 10.91 (s, 1H); $^{13}C\{^1H\}$ NMR (100 MHz) δ 8.8, 9.0, 9.9, 10.5, 14.6, 25.5, 29.0, 29.8, 42.2, 49.8, 53.0, 60.0, 64.5, 106.8, 107.7, 115.8, 117.3, 120.4, 120.6, 121.2, 124.3, 126.7, 126.8, 126.9, 128.8, 131.2, 136.1, 136.9, 138.7, 139.9, 141.3, 161.8, 163.2, 165.5, 170.3, 188.0; ESI-MS m/z: $[M + H]^+$ calcd for $C_{36}H_{39}N_6O_5$ 635.29674; found 635.2962. UV-Vis λ_{max} (MeCN) (ε) 243 (26 000), 278 (22 000), 403 (34 000) and 469 (nm) (12 000 M^{-1} cm^{-1}).

Phyllobilin (8). Following a reported procedure[14] with modification, a sample of **7** (21.9 mg, 34.5 μmol) in anhydrous CH_3CN (175 mL) was treated with $Yb(OTf)_3$ (21.7 mg, 34.5 μmol) and stirred at 80 °C (oil bath) for 80 min under argon. Then, the reaction mixture was allowed to cool to room temperature and concentrated. The crude mixture was diluted with ethyl acetate (100 mL) and washed with saturated aqueous $NaHCO_3$ and then brine. The organic layer was dried (Na_2SO_4) and concentrated. Chromatography [silica, hexanes/ethyl acetate (1 : 1)] afforded an orange solid (10.3 mg, 46%): mp 135–140 °C dec.; ^{1}H NMR (700 MHz, CD_2Cl_2) δ 1.25 (s, 3H), 1.27 (s, 3H), 1.34–1.36 (t, J = 7 Hz, 3H), 1.98 (s, 3H), 2.05 (s, 3H), 2.12 (s, 3H), 2.26 (s, 3H), 2.42–2.44 (d, J = 16.8 Hz, 1H), 2.53–2.55 (d, J = 17.5 Hz, 1H), 3.70 (s, 3H), 3.75 (s, 2H), 4.20 (s, 1H), 4.23–4.25 (d, J = 15.4 Hz, 2H), 4.28–4.31 (q, J = 7 Hz, 2H), 6.14 (s, 1H), 7.36 (s, 1H), 9.87 (s, 1H), 10.16 (s, 1H), 10.05 (s, 1H), 11.37 (s, 1H); $^{13}C\{^1H\}$ NMR (150 MHz, CD_2Cl_2) δ 9.0, 9.2, 10.1, 10.9, 14.7, 24.9, 25.8, 25.9, 26.3, 30.3, 42.6, 50.9, 53.0, 61.2, 62.0, 64.4, 102.1, 114.5, 116.8, 117.6, 117.9, 120.8, 124.8, 126.7, 128.8, 129.3, 137.3, 138.9, 141.8, 141.9, 147.2, 154.6, 164.9, 169.3, 186.4, 189.4; ESI-MS m/z: $[M + H]^+$ calcd for $C_{36}H_{38}N_6O_5$ 635.2976; found 635.2957. UV-Vis λ_{max} (MeCN) (ε) 237 (14 000), 280 (15 000), 357 (20 000) and 403 (nm) (26 000 M^{-1} cm^{-1}).

Conflicts of interest

The authors declare no competing financial interests.

Acknowledgements

This work was supported by the NSF (CHE-1760839, CHE-2054497). NMR spectroscopy and mass spectrometry measurements were carried out in the Molecular Education, Technology, and Research Innovation Center (METRIC) at NC State University. Single-crystal X-ray diffraction data were obtained at

the University of Tennessee at Knoxville (by Dr Phattananawee Nalaoh). Computing resources were provided by North Carolina State University High Performance Computing Services Core Facility (RRID:SCR_022168). This work used Bridges-2 at Pittsburgh Supercomputing Center through allocation [CHE240037] from the Advanced Cyberinfrastructure Coordination Ecosystem: Services & Support (ACCESS) program, which is supported by National Science Foundation grants #2138259, #2138286, #2138307, #2137603, and #2138296.

References

1 G. A. F. Hendry, J. D. Houghton and S. B. Brown, *New Phytol.*, 1987, **107**, 255–302.
2 B. Kräutler, *Chem. Soc. Rev.*, 2014, **43**, 6227–6238.
3 P. Wang, C. A. Karg, N. Frey, J. Frädrich, A. M. Vollmar and S. Moser, *Arch. Pharm.*, 2021, **354**, e2100061.
4 C. A. Karg, M. Taniguchi, J. S. Lindsey and S. Moser, *Planta Med.*, 2023, **89**, 637–662.
5 T. Müller, M. Ulrich, K. Ongania and B. Kräutler, *Angew. Chem., Int. Ed.*, 2007, **46**, 8699–8702.
6 C. A. Karg, L. Parráková, D. Fuchs, H. Schennach, B. Kräutler, S. Moser and J. M. Gostner, *Antioxidants*, 2022, **11**, 2056.
7 M. Roca, *Food Chem.*, 2012, **130**, 134–138.
8 C. A. Karg, C. Doppler, C. Schilling, F. Jakobs, M. C. S. Dal Colle, N. Frey, D. Bernhard, A. M. Vollmar and S. Moser, *Food Chem.*, 2021, **359**, 129906.
9 C. A. Karg, P. Wang, F. Kluibenschedl, T. Müller, L. Allmendinger, A. M. Vollmar and S. Moser, *Eur. J. Org. Chem.*, 2020, 4499–4509.
10 C. A. Karg, S. Wang, N. Al Danaf, R. P. Pemberton, D. Bernard, M. Kretschmer, S. Schneider, T. Zisis, A. M. Vollmar, D. C. Lamb, S. Zahler and S. Moser, *Angew. Chem., Int. Ed.*, 2021, **60**, 22578–22584.
11 C. A. Karg, P. Wang, A. M. Vollmar and S. Moser, *Phytomedicine*, 2019, **60**, 152969.
12 I. Schumacher, D. Menghini, S. Ovinnikov, M. Hauenstein, N. Fankhauser, C. Zipfel, S. Hörtensteiner and S. Aubry, *Plant J.*, 2022, **109**, 1473–1488.
13 Y. Liu, S. Zhang and J. S. Lindsey, *Nat. Prod. Rep.*, 2018, **35**, 879–901.
14 S. Zhang and J. S. Lindsey, *J. Org. Chem.*, 2017, **82**, 2489–2504.
15 P. Wang, F. Lu and J. S. Lindsey, *J. Org. Chem.*, 2020, **85**, 702–715.
16 K. Chau Nguyen, P. Wang, R. D. Sommer and J. S. Lindsey, *J. Org. Chem.*, 2020, **85**, 6605–6619.
17 D. T. M. Chung, P. V. Tran, K. Chau Nguyen, P. Wang and J. S. Lindsey, *New J. Chem.*, 2021, **45**, 13302–13316.
18 K. Chau Nguyen, A. T. Nguyen Tran, P. Wang, S. Zhang, Z. Wu, M. Taniguchi and J. S. Lindsey, *Molecules*, 2023, **28**, 1323.
19 K. Chau Nguyen and J. S. Lindsey, *J. Org. Chem.*, 2023, **88**, 11205–11216.
20 A. T. Nguyen Tran, Z. Wu, D. T. M. Chung, P. Nalaoh and J. S. Lindsey, *New J. Chem.*, 2023, **47**, 13626–13637.
21 H. Fischer and M. Neber, *Justus Liebigs Ann. Chem.*, 1932, **496**, 1–26.
22 M. E. Flaugh and H. Rapoport, *J. Am. Chem. Soc.*, 1968, **90**, 6877–6879.
23 R. B. Woodward, W. A. Ayer, J. M. Beaton, F. Bickelhaupt, R. Bonnett, P. Buchschacher, G. L. Closs, H. Dutler, J. Hannah, F. P. Hauck, S. Itŏ, A. Langemann, E. Le Goff, W. Leimgruber, W. Lwowski, J. Sauer, Z. Valenta and H. Volz, *Tetrahedron*, 1990, **46**, 7599–7659.
24 Y. Joh and K. Makino, *Jikeikai Med. J.*, 1971, **18**, 121–131.
25 J. B. Paine III, R. B. Woodward and D. Dolphin, *J. Org. Chem.*, 1976, **41**, 2826–2835.
26 T. P. Wijesekera, J. B. Paine III and D. Dolphin, *J. Org. Chem.*, 1985, **50**, 3832–3838.
27 B. Morgan and D. Dolphin, *Angew. Chem., Int. Ed. Engl.*, 1985, **24**, 1003–1004.
28 B. Morgan, D. Dolphin, R. H. Jones, T. Jones and F. W. B. Einstein, *J. Org. Chem.*, 1987, **52**, 4628–4631.
29 B. Morgan and D. Dolphin, *J. Org. Chem.*, 1987, **52**, 5364–5374.
30 C. Haubmann, H. Hübner and P. Gmeiner, *Bioorg. Med. Chem. Lett.*, 1999, **9**, 1969–1972.
31 L. Y. Xie, R. W. Boyle and D. Dolphin, *J. Am. Chem. Soc.*, 1996, **118**(20), 4853–4859.
32 S. David, D. Dolphin, B. R. James, J. B. Paine III, T. P. Wijesekera, F. W. B. Einstein and T. Jones, *Can. J. Chem.*, 1986, **64**, 208–212.
33 T. P. Wijesekera, J. B. Paine III and D. Dolphin, *J. Org. Chem.*, 1988, **53**, 1345–1352.
34 D. Dolphin, S. J. Rettig, H. Tang, T. Wijesekera and L. Y. Xie, *J. Am. Chem. Soc.*, 1993, **115**, 9301–9302.
35 R. W. Boyle, V. Karunaratne, A. Jasat, E. K. Mar and D. Dolphin, *Synlett*, 1994, 939–940.
36 L. Y. Xie and D. Dolphin, *J. Chem. Soc., Chem. Commun.*, 1994, 1475–1476.
37 T. Okawara, R. Kawano, H. Morita, A. Finkelstein, R. Toyofuku, K. Matsumoto, K. Takehara, T. Nagamura, S. Iwasa and S. Kumar, *Molecules*, 2017, **22**, 1816.
38 B. Jolicoeur, E. E. Chapman, A. Thompson and W. D. Lubell, *Tetrahedron*, 2006, **62**, 11531–11563.
39 E. Bullock, A. W. Johnson, E. Markham and K. B. Shaw, *J. Chem. Soc.*, 1958, 1430–1440.
40 H. Falk, O. Hofer and H. Lehner, *Monatsh. Chem.*, 1973, **104**, 925–932.
41 J. B. Paine III and D. Dolphin, *Can. J. Chem.*, 1976, **54**, 411–414.
42 G. Jones, *Org. React.*, 1967, **15**, 204–599.
43 B. List, *Angew. Chem., Int. Ed.*, 2010, **49**, 1730–1734.
44 S. Zhang, M. N. Reddy, O. Mass, H.-J. Kim, G. Hu and J. S. Lindsey, *New J. Chem.*, 2017, **41**, 11170–11189.
45 T. Mietke, T. Cruchter, V. A. Larionov, T. Faber, K. Harms and E. Meggers, *Adv. Synth. Catal.*, 2018, **360**, 2093–2100.
46 Z. A. Krasnaya, I. V. Torgov and N. S. Prostakov, *Herald Russ. Acad. Sci.*, 2006, **76**, 370–375.

47 T. Vaidya, R. Eisenberg and A. J. Frontier, *ChemCatChem*, 2011, **3**, 1531–1548.
48 F. Neese, *WIREs Comp. Mol. Sci.*, 2022, **12**, e1606.
49 J. P. Perdew, M. Ernzerhof and K. Burke, *J. Chem. Phys.*, 1996, **105**, 9982–9985.
50 F. Weigend and R. Ahlrichs, *Phys. Chem. Chem. Phys.*, 2005, **7**, 3297–3305.
51 F. Weigend, *Phys. Chem. Chem. Phys.*, 2006, **8**, 1057–1065.
52 F. Neese, F. Wennmohs, U. Becker and C. Riplinger, *J. Chem. Phys.*, 2020, **152**, 224108.
53 S. E. Boiadjiev and D. A. Lightner, *Tetrahedron: Asymmetry*, 1999, **10**, 607–655.
54 H. H. Strain and W. M. Manning, *J. Biol. Chem.*, 1942, **146**, 275.
55 A. S. Holt and E. E. Jacobs, *Plant Physiol.*, 1955, **30**, 553–559.
56 J. L. Burdett and M. T. Rogers, *J. Am. Chem. Soc.*, 1964, **86**, 2105–2109.
57 M. Nsangou, A. B. Fredj, N. Jaïdane, M. G. Kwato Njock and Z. B. Lankhdar, *J. Mol. Struct.: THEOCHEM*, 2004, **681**, 213–224.
58 J. J. Ríos, M. Roca and A. Pérez-Gávez, *J. Agric. Food Chem.*, 2014, **62**, 10576–10584.
59 B. Kräutler and S. Hörtensteiner, in Chlorophylls and Bacteriochlorophylls. Biochemistry, Biophysics, Functions and Applications, ed. B. Grimm, R. J. Porra, W. Rüdiger and H. Scheer, *Advances in Photosynthesis and Respiration*, Springer: Dordrecht, The Netherlands, 2006, vol. 25, pp. 237–260.
60 M. Oberhuber, J. Berghold and B. Kräutler, *Angew. Chem., Int. Ed.*, 2008, **47**, 3057–3061.
61 B. Kräutler, in *Tetrapyrroles: Birth, Life and Death*, ed. M. J. Warren and A. G. Smith, Landes Bioscience: Austin, TX, 2009, pp. 274–285.
62 I. Süssenbacher, S. Hörtensteiner and B. Kräutler, *Angew. Chem., Int. Ed.*, 2015, **54**, 13777–13781.